Int J Clin Exp Med 2019;12(1):1206-1216
www.ijcem.com /ISSN:1940-5901/IJCEM0076964

Original Article

MicroRNA-564 acts as a tumor suppressor by directly targeting CDK16 in bladder carcinoma cell lines

Zhe Zhang[1], Liangtong Li[1], Ning Zhu[2], Huiqin Wang[2]

[1]Medical College, Hebei University, Baoding 071002, Hebei, China; [2]Department of Cardiology, Baoding First Center Hospital, Baoding 071002, Hebei, China

Received July 30, 2017; Accepted October 20, 2018; Epub January 15, 2019; Published January 30, 2019

Abstract: Objective: MicroRNAs (miRNAs) are small non-coding RNAs contributes to the development and progression of many type cancers including retinoblastoma at the post-transcriptional level. However, the role of miR-564 in bladder cancer remains to be elucidated. In the present study, we aimed to explore the regulatory mechanism of miR-564 in bladder cancer cell proliferation and migration. Methods: MTT was used to detect the cell viability. Transwell assay was used to detect the cell migration. Quantitative realtime PCR was used to evaluate the gene expression. Western blot was used to detect the protein expression. Flow cytometry was carried out to analyze the cell cycle. Luciferase activity assay was used to confirm whether miR-564 target CDK16. Results: MiR-564 was found down-regulated in the bladder cancer tissues and cell lines. Over-expression of miR-564 significantly inhibited the bladder cancer cell proliferation and migration and induced cell cycle arrest. Luciferase activity assay and rescue experiment confirmed that miR-564 directly targets CDK16 in bladder cancer cells. At last, we analyzed the relation between miR-564 and CDK16 in bladder cancer cell, the results showed a negative correlation between miR-564 and CDK16. Conclusion: MiR-564 may act as a tumor suppressor that could serve as a key role in the diagnosis and treatment of bladder cancer.

Keywords: miR-564, CDK16, bladder cancer, tumorigenesis

Introduction

Bladder carcinoma (BC) is the most common malignancy of the urinary tract with about 386,300 new cases and 150,200 deaths annually [1, 2]. Despite significant advances in accurate and effective diagnostic and therapeutic methods, bladder cancer is still a highly prevalent and lethal malignancy [3]. It has been demonstrated that dysregulation of certain tumor related genes contributes to the proliferation, invasion and metastasis of bladder cancer largely. Accordingly, therapy point at gene-targeted therapy has been recommended as a reasonable strategy for bladder cancer treatment. However, the pathogenesis of bladder cancer is complicated, which is the result of the interaction of multiple factors include heredity, environment, and metabolism factors. Moreover, the precise causes and pathogenesis of bladder cancer remain poorly understood, making it urgent to understand the molecular mechanisms of the progression of bladder cancer.

miRNAs are a class of small, non-coding RNAs that regulate approximately 30% of all genes and protein expression negatively at the post-transcriptional level. Therefore, miRNAs are necessary for the regulation of numerous processes, including cell growth, differentiation and apoptosis. Aberrant miRNA expression has been frequently observed in various types of human tumors [4-8]. Among these, miR-564 has been demonstrated to be down-regulated in many malignancies [8, 9]. It has been indicated that miR-564 functions as a tumor suppressor in human lung cancer by targeting ZIC3. However, little is known about the influence of miR-564 on bladder cancer [10].

In the present study, we aimed to explore the expression alteration of miR-564 in human bladder cancer tissues and cell lines and the effect of miR-564. Moreover, we need to investiate the underlying mechanism involved in the initiation and development of human bladder cancer.

Materials and methods

Human tissue samples

Tissue specimens and the paired noncancerous bladder tissues used in this study were obtained from The NO. 2 Hospital of Tianjin Medical University (Tianjin, China) after surgical resection. All samples were immediately snapped frozen in liquid nitrogen and stored at -80°C for the following experiments. Informed consents were obtained from each patient to approve the use of their tissues for research purposes. The study protocol was approved by the Institute Research Ethics Committee of the NO.2 Hospital of Tianjin Medical University.

Cell culture and transfection

Hcv29 cell (Human bladder epithelial cell), Hbc (established by the Cancer Research Institute of Kunming Medical College, 1986), human bladder cancer cell lines (BIU-87 and T24) were cultured in RPMI-1640 (Invitrogen, CA, USA), UM-UC3 cell was cultured in MEM (Invitrogen, CA, USA) medium supplemented with 10% fetal bovine serum (Gibco, Australia), penicillin and streptomycin (100 IU/ml) at 37°C under a 5% CO_2 atmosphere in a humidified incubator. The CDS sequence of CDK16 was synthesized by Genewiz (Beijing, China) and cloned into pcDNA3.1 (+) vector (Promeaga, WI, USA) at BamHI and HindIII site. Bladder cancer cells (T24 and Hbc) were cultured at 3×10^4 cells/well in 96-well plates or 5×10^5 cells/well in 6-well plates until reaching 80% confluence. Subsequently, cells were transiently transfected with miRNA-564 mimics (Sense: 5' AGGCACGGUGUCAGCAGGCTT 3', Antisense: 5' TTUCCGUGCCACAGUCGUCCG 3'), mirRNA-564 inhibitors (5' UCCGUGCCACAGUCGUCCG 3') (genepharma, shanghai, China) or pcDNA3.1 (+)/CDK16 vector using Lipofectamine 2000 (Invitrogen, CA, USA) according to the manufacturer's instructions. To ensure actual transfection, qRT-PCR was carried out to detect transfection efficiencies in every experiment 24 hours later.

Realtime-PCR analysis

Total RNA was extracted using Trizol reagent (Invitrogen, CA, USA) according to the instructions. cDNA was synthesized with specific stem-loop primers and the TaqMan MicroRNA Reverse Transcription Kit (Applied Biosystems, CA, USA). The levels of gene expression were quantified on an iQ5 real-time PCR detection system (Bio-Rad, MA, USA) with SYBR Premix EX Taq (TaKaRa, Shiga, Japan). The expression of miR-564 and CDK16 was defined based on the threshold cycle (Ct) normalized to that of the housekeeping gene GAPDH or small nuclear RNA U6 as internal controls. The fold change of gene expression was calculated with the $2^{-\Delta\Delta Ct}$ method. PCR amplification was carried out using the following thermal conditions: 95°C for 30 s followed by 38 cycles of 95°C for 5 s and 60°C for 30 s. The PCR conditions for amplification of miR-564 were as follows: 95°C for 20 s, 38 cycles of 95°C for 10 s and 60°C for 20 s, with a final incubation at 70°C for 5 s. All the primers were synthesized by Genewiz (Beijing, China) and the sequence were as followed: miR-564 forward: ACACTCCAGCTGGGAGGCACGGTGTCA, miR-564 reverse: TGGTGTCGTGGAGTCG; CDK16 forward: GCA CGA GGA CTT GAA GAT GG, CDK16 reverse: CGCATACGCACTCTCACTG; U6 forward: CTCGCTTCGGCAGCACA, U6 reverse: AACGCTTCACGAATTTGCGT; GAPDH forward: CGCTCTCTGCTCCTCCTGTTC, GAPDH reverse: ATCCGTTGACTCCGACCTTCAC.

Cell viability assay

T24 and Hbc cells were plated at 3×10^4/well in 96-well plates. 24 h later, cells were transfected with miR-564 mimics, miR-564 inhibitor and controls. WST-8 staining with Cell Counting Kit-8 (Beyotime, Haimen, China) was performed to detect the cell proliferation at 24, 48, 72 and 96 hours after transfection.

Western blot assay

Protein was extracted from T24 and Hbc cells using (20 mM Tris pH 7.5, 150 mM NaCl, 1% Triton X-100, sodium pyrophosphate, β-glycerophosphate, EDTA, Na3VO4, leupeptin, Beyotime, Haimen, China). The protein lysate was separated on a 10% SDS-PAGE gel and then transferred to PVDF membranes (Bio-Rad, CA, USA). Nonspecific binding was blocked by incubating the PVDF membranes with 5% nonfat milk containing 0.1% Tween-20 for 2 hours at room temperature. The membrane was incubated Primary antibodies included CDK16 (Abcam, cambridge, England), and GAPDH (Abcam, cambridge, England) in TBST at 4°C

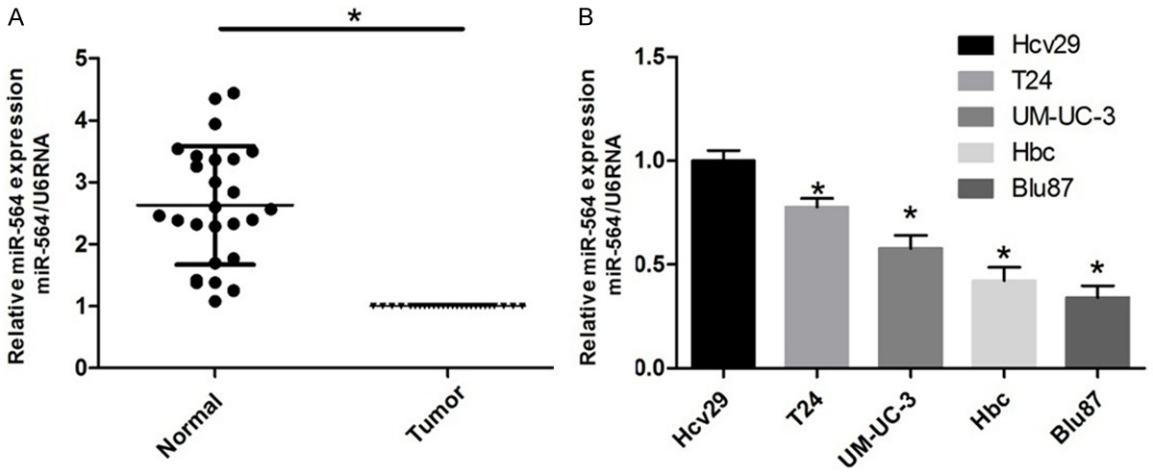

Figure 1. The aberrent expression of miR-564 in bladder carcinoma and cell lines. A. Realtime-PCR was used to investigate the expression of miR-564 in bladder carcinomas and the paired adjacent normal tissues. B. Realtime-PCR was used to investigate the expression of miR-564 in bladder cancer cell lines (T24 and Hbc) and in the normal Hcv29 cell. Bars represent the mean ± SD of three independent experiments. **P<0.01, *P<0.05.

overnight. After washing with TBST for three times, the PVDF membranes were incubated with horseradish peroxidase-conjugated sheep anti-mouse IgG for 2 h at 37°C. Finally, the proteins were visualized using ECL detection kits (Millipore, MA, USA).

Luciferase assay

The oligonucleotide with wide type or mutant type 3'-UTR region of CDK16 (containing binding site with miR-564) were synthesized by Genewiz (Beijing, China). The pmiRGLO vectors (Promeaga, WI, USA) were constructed with wild type CDK16 sequences or mutant CDK16 sequences. T24 and Hbc cells were seeded in 12-well plates and subsequently co-transfected with miR-control/miR-214 mimics and WT-CDK16 3'-UTR vector/mut-CDK16 3'-UTR vector using Lipofectamine 2000 (Invitrogen, CA, USA) following the manufacture's instructions. The activities of Renilla and firefly luciferases were measured using the Dual-Luciferase assay kit (Promega, WI, USA).

Colony formation assay

500 Cells 24 h after transfection were seeded into 6-well plates and cultured for 14 days. After there, cells were subsequently fixed with absolute methanol for 15 min and stained with crystal violet for 20 min. The number of colonies formed was counted in 8 different fields of vision. Each experiment was performed independently for three times.

Cell migration assay

48 h after transfection, cells were trypsinized and seeded in 8 μm pore size transwell chambers (Corning, Cambridge, USA) at the density of 8×104 per well and cultured in RPMI 1640 medium with 2% FBS, while 600 μl of RPMI-1640 supplemented with 10% FBS was added to the lower chamber. 24 hours later, migrated cells were fixed with absolute methanol for 30 min. Non-migrated cells were removed by cotton swabs. Then cells on bottom surface of the membrane were stained by 0.1% crystal violet. Five visual fields of ×200 magnification of each insert were randomly selected, and the number of cells was counted under a light microscope.

Cell cycle analysis

24 h after transfection, cells (1×106) were harvested and fixed in 75% ice-cold ethanol. Fixed cells were treated with bovine pancreatic containing 2 μg/ml RNase (Sigma, CA, USA) for 25 min, and followed by incubating in 20 μg/ml propidium iodide (Sigma, CA, USA) for 20 min. Cell cycle analysis was performed on a FACS-Calibur System (BD Biosciences, NJ, USA). The data were analyzed with the flowjo software and the cell cycle distribution was shown as the percentage of cells in the G0/G1, S, and G2/M

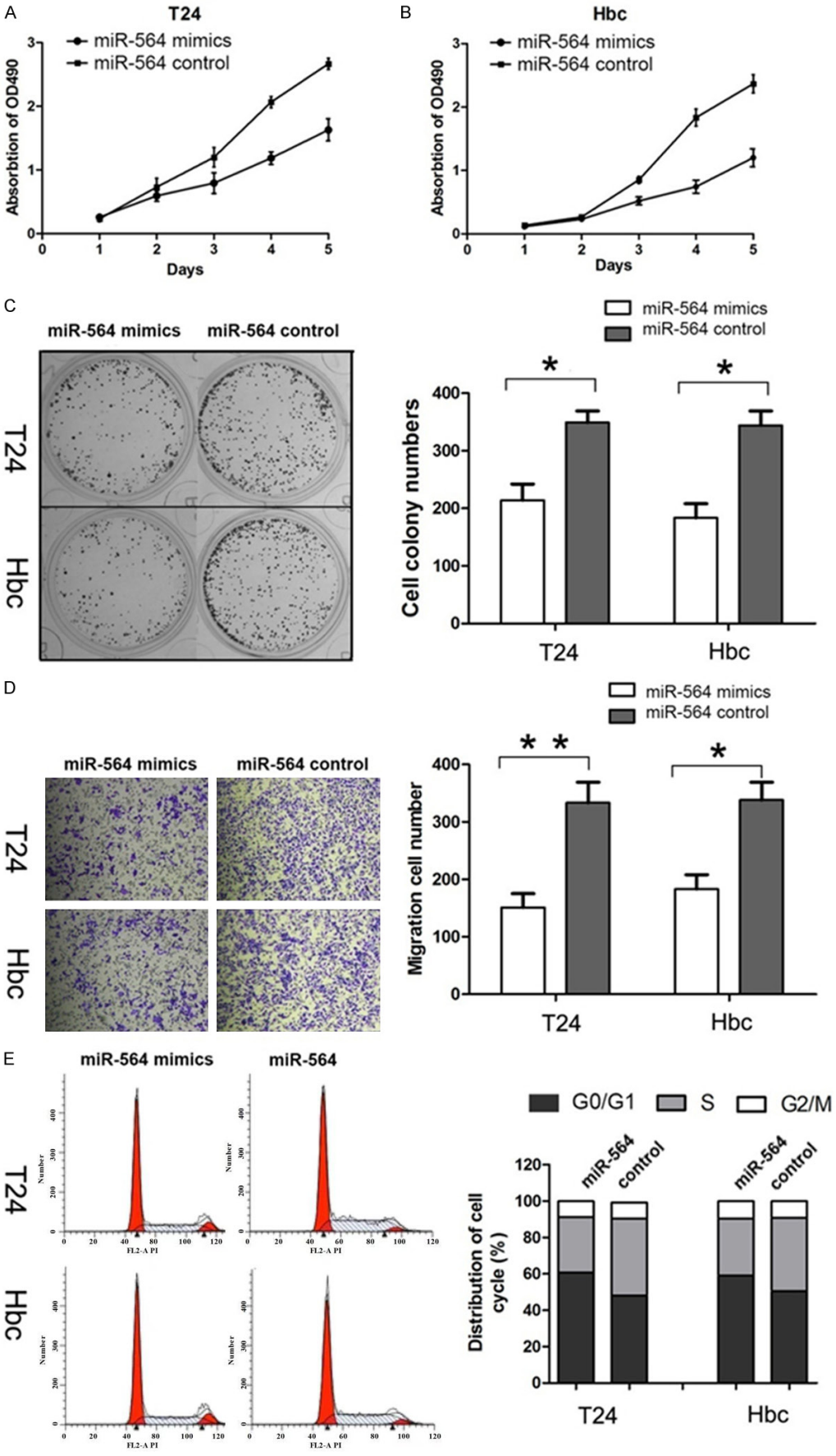
A
T24
miR-564 mimics
miR-564 control
Absorbtion of OD490
Days
B
Hbc
miR-564 mimics
miR-564 control
Absorbtion of OD490
Days
C
miR-564 mimics
miR-564 control
T24
Hbc
miR-564 mimics
miR-564 control
Cell colony numbers
T24
Hbc
D
miR-564 mimics
miR-564 control
T24
Hbc
miR-564 mimics
miR-564 control
Migration cell number
T24
Hbc
E
miR-564 mimics
miR-564
T24
Hbc
Number
FL2-A PI
G0/G1
S
G2/M
miR-564
control
miR-564
control
Distribution of cell cycle (%)
T24
Hbc

Figure 2. MiR-564 attenuated bladder cancer cell growth and induced cell cycle arrest. A, B. MTT assay was performed every 24 h until 96 h after transfection and proliferation curves of T24 and Hbc cells were depicted respectively. C. Representative micrographs (left) and quantifications (right) of crystal violet stained colonies formed by the indicated cells. D. Cell migration of the indicated cells in a transwell cell migration assay, shown by quantification and representative images. E. PI staining and flow cytometry were used to analysis the cell cycle distribution of T24 and Hbc cells. Bars represent the mean ± SD of three independent experiments. **P<0.01, *P<0.05.

populations. Each experiment was carried out in triplicate.

Statistical analysis

All statistical analyses and graphing were performed using SPSS version 17.0. The data were expressed as the mean ± standard deviation (SD) for three independent experiments. Student's t-test was used to evaluate the significant difference of two groups of data in all the pertinent experiments. Multiple variances were analyzed by two-way ANOVA. *P* value <0.05 was regarded as statistically significant.

Results

MiR-564 was down-regulated in bladder cancer tissues and cell lines

qPCR was used to evaluate the miR-564 expression in bladder cancer tissues and the adjacent normal tissues along with the bladder cancer cell lines and Hcv9 cell. The results demonstrated that miR-564 expression was markedly lower in bladder cancer tissues and cell lines than that in adjacent normal tissues and Hcv29 cells (**Figure 1A**, **1B**).

miR-564 attenuated bladder cancer cells proliferation and induced cell cycle progression

T24 and Hbc cells were transfected with miR-564 mimics for 48 h. MTT assay was performed following the procedure described in methods every 24 hour and proliferation curve was depicted. The results revealed that miR-564 resulted in significantly decreased cell viability at 96 h and 120 h in both T24 and Hbc cells (**Figure 2A**, **2B**). Similar trends were also observed in colony formation rate. MiR-564 over-expression led to a significantly lower colony formation rate (**Figure 2C**) in T24 and Hbc cells. In addition, cell migration assay was performed to further investigate the role of miR-564 in bladder cancer cells. As expected, transfection of miR-564 mimics significantly reduced the migration cell number in both T24 and Hbc cells (**Figure 2D**). The cell cycle analysis of T24 and Hbc cells by flow cytometry showed a significant cut down in the percentage of cells in G1/G0 phase and an increase in the percentage of cells in S phase (**Figure 2E**). These results indicated that over-expression of miR-564 inhibited the proliferation, migration and cell cycle progression of bladder cancer cells *in vitro*.

Knock-down of miR-564 promoted the proliferative capacity of bladder cancer cells

Loss-of-function study was performed using a miR-564 inhibitor to further confirm whether inhibition of miR-564 reduces bladder cancer cell proliferation. MTT and colony formation assays revealed that inhibition of miR-564 significantly increased the proliferative capacity of T24 and 5637 cells compared with cells transfected with NC (**Figure 3A-C**). The migration assay revealed that suppression of miR-564 led to an elevated migration cell number (**Figure 3D**). Flow cytometry showed a significant decrease in the percentage of cells in G1/G0 phase and a rise in the percentage of cells in S phase in cells transfected with the miR-564 inhibitor in comparison with NC transfected cells (**Figure 3E**). These results suggested that down-regulation of miR-564 facilitated the proliferation and cell cycle progression of bladder cancer cells.

MiR-564 directly targeted CDK16

MiRNAs execute post-transcriptional regulation mostly by binding to the 3'-UTR of the down-stream genes. Accordingly, we used bioinformatics prediction software Targetscan to find out the target which is involved in the regulation of cell growth capability, (http://http://www.targetscan.org/). Among these thousands of candidates, we focused on CDK16. Luciferase reporter assays was performed to verify an interaction between miR-564 and the 3'UTR of CDK16. The 3'UTR of CDK16 was cloned into down-stream of the pmirGLO Dual-Luciferase miRNA target expression vector. In

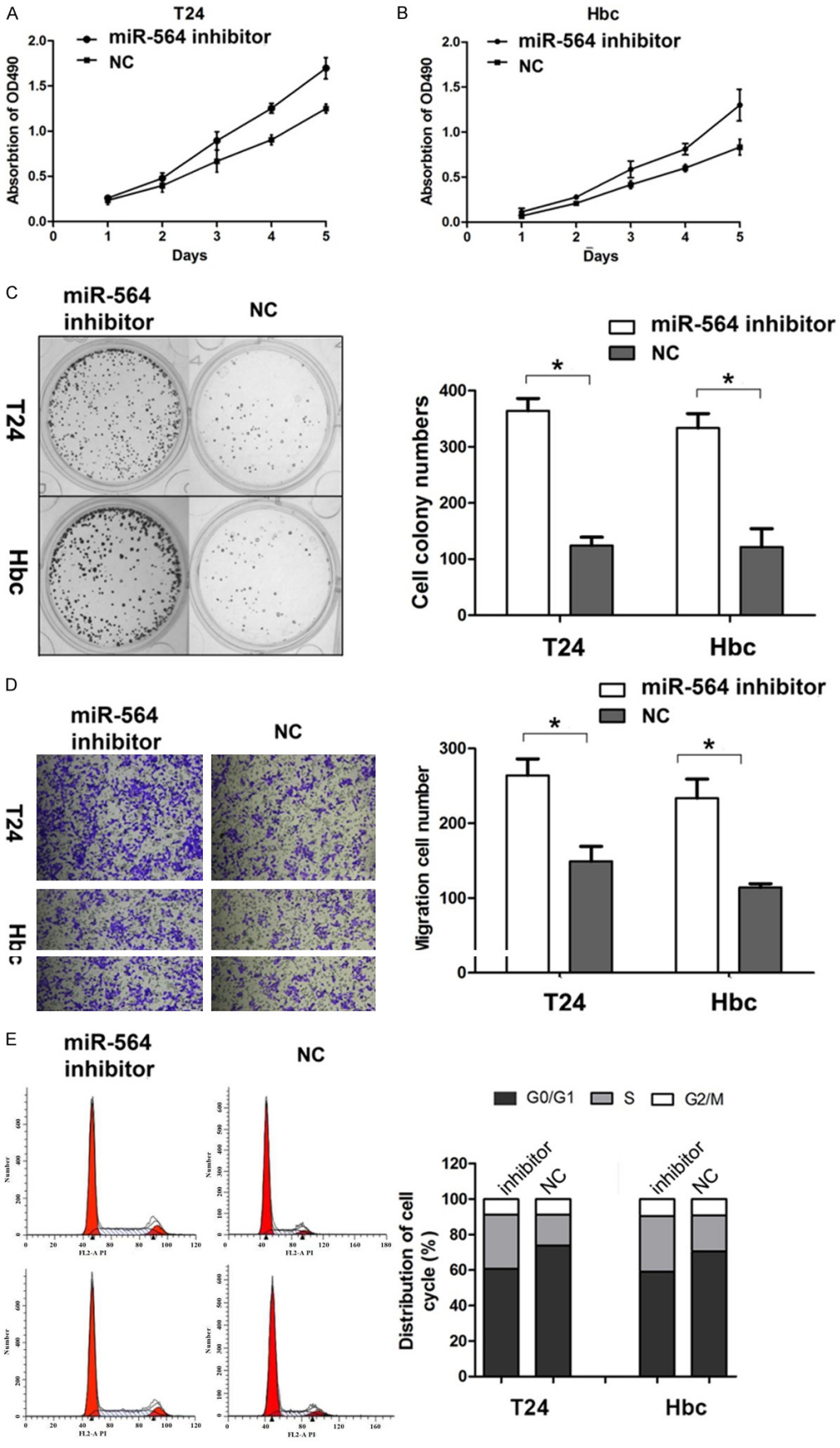
A
T24
miR-564 inhibitor
NC
Absorbtion of OD490
Days
B
Hbc
miR-564 inhibitor
NC
Absorbtion of OD490
Days
C
miR-564 inhibitor
NC
T24
Hbc
miR-564 inhibitor
NC
Cell colony numbers
T24
Hbc
D
miR-564 inhibitor
NC
T24
Hbc
miR-564 inhibitor
NC
Migration cell number
T24
Hbc
E
miR-564 inhibitor
NC
G0/G1
S
G2/M
inhibitor
NC
inhibitor
NC
Distribution of cell cycle (%)
T24
Hbc

Figure 3. Inhibition of miR-564 promoted bladder cancer cell growth and cell cycle progression. A, B. MTT assay was performed every 24 h until 96 h after transfection and proliferation curves of T24 and Hbc cells were depicted respectively. C. Representative micrographs (left) and quantifications (right) of crystal violet stained colonies formed by the indicated cells. D. Cell migration of indicated cells in a transwell cell migration assay, shown by quantification and representative images. E. PI staining and flow cytometry were used to analysis the cell cycle distribution of T24 and Hbc cells. Bars represent the mean ± SD of three independent experiments. **P<0.01, *P<0.05.

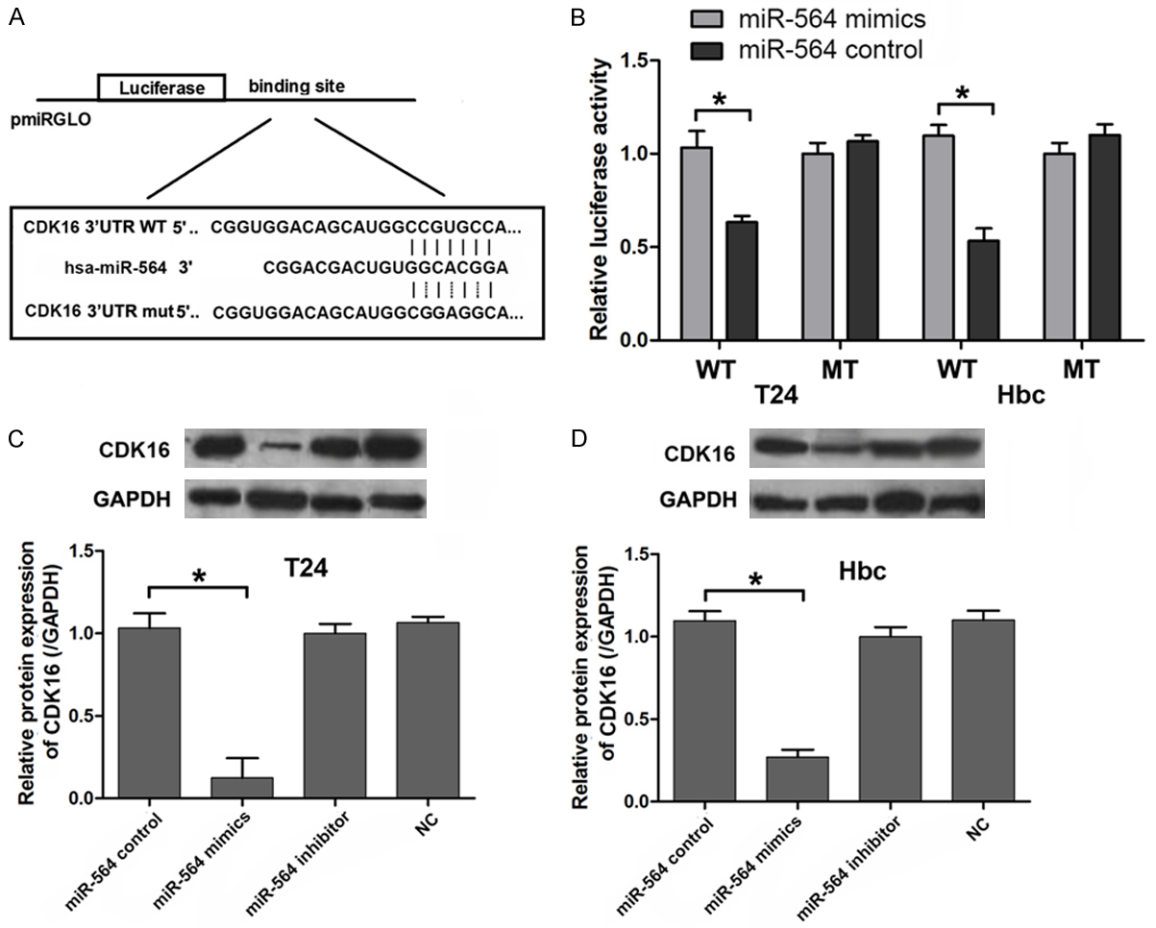

Figure 4. MiR-564 target the 3'UTR of CDK16 mRNA directly. A. Bioinformatics analyses of the binding of miR-564 to the 3'-UTR of CDK16 mRNA. B. Luciferase report assay was carried out to determine whether CDK16 was a target of miR-564. C, D. Western blot analysis was used to determine the protein level of CDK16 in T24 and Hbc cells transfected with miR-564 mimic or miR-195 inhibitor, respectively. GAPDH was used as an endogenous reference. Bars represent the mean ± SD of three independent experiments. **P<0.01, *P<0.05.

addition, a mutated CDK16 3'-UTR vector was also constructed (**Figure 4A**). Co-transfection of the wt-3'-UTR-reporter and miR-564 showed significantly decreased relative luciferase activity compared with cells transfected with miR-564 control. However, the luciferase activity of the reporter carrying 3'-UTR with mutated binding sites was unaffected by the co-transfection with miR-564 (**Figure 4B**). These results strongly indicated that the CDK16 was the direct target of miR-564.

Over-expression of CDK16 reversed the effect of miR-564 on cell proliferation

Rescue experiment was carried out to further confirm the crucial effect of CDK16 during miR-564 inhibited bladder cancer proliferation. An over-expression vector pcDNA3.1 (+)/CDK16 was constructed to enhance the endogenous CDK16 expression. The results of cell MTT and the colony formation assay both indicated that the proliferation suppressing effect of miR-564

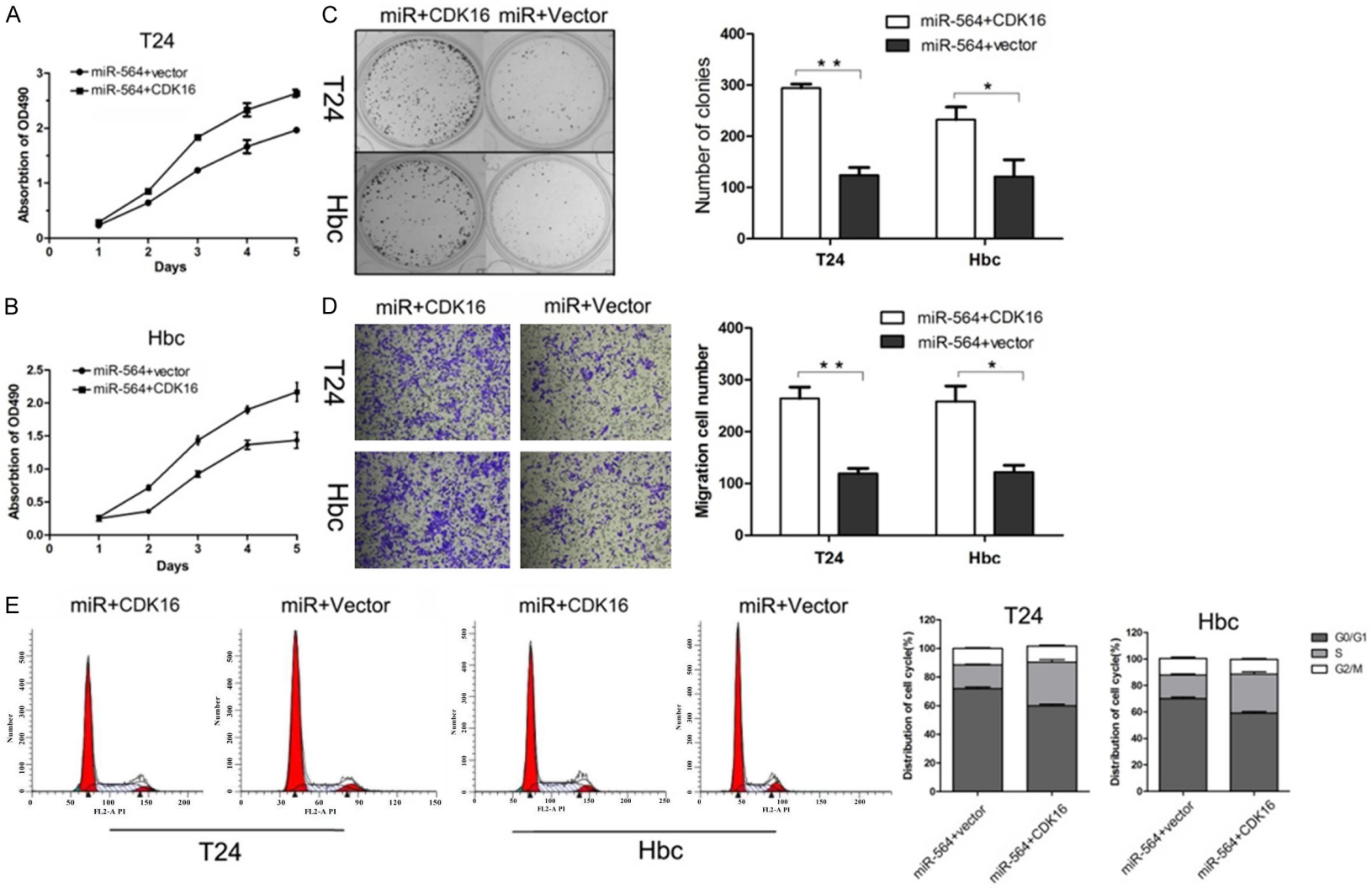

Figure 5. Rescue experiment was applied to confirm CDK16 as a target of MiR-564. A, B. MTT assay was performed every 24 h until 96 h after co-transfection with miR-564 mimics and CDK16 overexpression vector or with miR-564 and control vector and proliferation curves were depicted respectively. C. Representative micrographs (left) and quantifications (right) of crystal violet stained colonies formed by the T24 and Hbc cells co-transfected with miR-564 mimics and CDK16 overexpression vector or with miR-564 and control vector. D. Cell migration of T24 and Hbc cells under indicated treatments in a transwell cell migration assay, shown by quantification and representative images. E. PI staining and flow cytometry were used to analysis the cell cycle distribution of T24 and Hbc cells under indicated treatments. Bars represent the mean ± SD of three independent experiments. **P<0.01, *P<0.05.

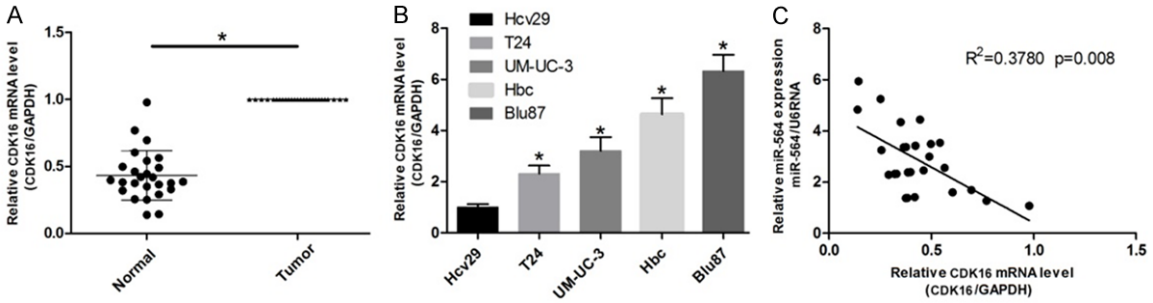

Figure 6. The aberrent expression of CDK16 in bladder carcinoma and cell lines. A, B. Realtime-PCR was used to investigate the expression of CDK16 in bladder carcinomas and the paired adjacent normal tissues as well as in bladder cell lines (T24 and Hbc) and in the normal Hcv29 cell. C. The correlation analysis was performed to evaluate the correlation between miR-564 and CDK16. Bars represent the mean ± SD of three independent experiments. **P<0.01, *P<0.05.

was reversed by CDK16 in both cells (**Figure 5A-C**). Migration assay indicated that CDK16 notably reversed miR-564's effect on the migration capability in T24 and Hbc cells (**Figure 5D**). Furthermore, cell cycle analysis demonstrated that CDK16 increased the cell proportion in S phase and reversed the effect of miR-564 on cell cycle progression (**Figure 5E**). These results suggested that over-expression of CDK16 could reverse the effect of miR-564 on bladder cancer cells proliferation and cycle progression.

CDK16 was up-regulated in bladder carcinoma and cell lines

qPCR was used to evaluate the expression of CDK16 in bladder cancer tissues and the adjacent normal tissues along with the bladder cancer cell lines and Hcv9 cell. We found that CDK16 expression was notably elevated in bladder cancer tissues and cell lines in comparison with the adjacent normal tissues and Hcv29 cell (**Figure 6A**, **6B**). To verify the relationship between CDK16 and miR-564, correlation analysis was carried out. As expected, CDK16 was negatively associated with miR-564 expression (**Figure 6C**).

Discussion

miRNAs play a key role in various tumor, data are emerging which elucidate the functions of miRNAs in bladder cancer [11-15].

In the current study, we found that miR-564 was significantly down-regulated in both bladder cancer tissues and cell lines indicating its potential function in pathogenesis of bladder cancer. As expected, *in vitro* functional studies revealed that miR-564 could inhibit cell viability, migration and colony formation rate, meanwhile induce G1 cell cycle arrest in bladder cancer cells. miRNAs function as post-transcriptional regulator by partially pairing with the 3'-UTR of target mRNAs, leading to mRNA degradation or translational repression. Previous report demonstrated miR-564 suppress lung cancer development by targeting ZIC3. In our work, integrated bioinformatics analysis (targetScan, picTar,) recognizes CDK16 as a miR-564 target gene.

CMGC protein kinase family includes cyclin-dependent kinases (CDKs), mitogen-activated protein kinases (MAPKs), glycogen synthase kinase, and CDK-like kinases [16-18]. CDK16 belongs to the CDK2 subfamily and is one of three members of the PCTAIRE family that contain a highly-conserved PSTAIRE motif which plays a key role in cyclin binding indicating that CDK16 may take part in cell cycle regulation and play a critical role during G1 to S phase transition [19-22]. A recent study reported that the CDK-16 mRNA and protein expression of was found significantly higher in serous epithelial ovarian cancer cells compared to normal control ovarian cells [23]. These findings CDK16 might be a part of cellular protein networks regulating cell cycle in cancer cells. Nevertheless, despite this well-conserved cyclin-binding motif CDK-16 has not been conclusively shown to be involved in cell cycle regulation. And CDK16 was only confirmed to be the direct target of miR-464. However, CDK16 was

down-regulated in nasopharyngeal carcinoma [24].

In our study, Dual-luciferase reporter assay showed that CDK16 had a miR-564 binding site in its 3'UTR. Moreover, CDK16 was inversely related to miR-564 expression in bladder cancer specimens. Over-expression of miR-564 attenuated CDK16 expression in both mRNA and protein levels, suggesting that miR-564 reduce CDK16 expression by degrading its mRNA. CDK16 knockdown recapitulated the effects of miR-564 over-expression, further illustrating that miR-564 directly targets CDK16. Whether the other members interact with miR-564 to play prominent roles in bladder cancer still need to be further verified in our future study.

Overall, miR-564 is a tumor suppressor in bladder cancer. miR-564-CDK16 axis is an important pathway modulating cell cycle, cell viability and proliferation of bladder cancer cells. However, the effects of miR-564 on the apoptosis or epithelial-mesenchymal transition (EMT) of bladder cancer cells have not been investigate. Further study is required to explore other deeper mechanisms of miR-564 in bladder cancer.

Acknowledgements

The research was supported by Health and Family Planning Commission of Hebei for Young Scientists (20120136).

Disclosure of conflict of interest

None.

Address correspondence to: Ning Zhu and Huiqin Wang, Department of Cardiology, Baoding First Center Hospital, 320 Changchengbeidajie, Baoding 071002, Hebei, China. Tel: +86 312 5976706; Fax: +86 312 5976586; E-mail: zhuning_my@126.com (NZ); huiqinwang1968@163.com (HQW)

References

[1] Jemal A, Bray F, Center MM, Ferlay J, Ward E, Forman D. Global cancer statistics. CA Cancer J Clin 2011; 61: 69-90.

[2] Griffiths TR. Current perspectives in bladder cancer management. Int J Clin Pract 2013; 67: 435-448.

[3] Shirodkar SP, Lokeshwar VB. Potential new urinary markers in the early detection of bladder cancer. Curr Opin Urol 2009; 19: 488-493.

[4] Liu Z, Mai C, Yang H, Zhen Y, Yu X, Hua S, Wu Q, Jiang Q, Zhang Y, Song X, Fang W. Candidate tumour suppressor CCDC19 regulates miR-184 direct targeting of C-Myc thereby suppressing cell growth in non-small cell lung cancers. J Cell Mol Med 2014; 18: 1667-1679.

[5] Gong B, Hu H, Chen J, Cao S, Yu J, Xue J, Chen F, Cai Y, He H, Zhang L. Caprin-1 is a novel microRNA-223 target for regulating the proliferation and invasion of human breast cancer cells. Biomed Pharmacother 2013; 67: 629-636.

[6] Yang Q, Wang Y, Lu X, Zhao Z, Zhu L, Chen S, Wu Q, Chen C, Wang Z. Mir-125b regulates epithelial-mesenchymal transition via targeting sema4C in paclitaxel-resistant breast cancer cells. Oncotarget 2015; 6: 3268-3279.

[7] Wang J, Raimondo M, Guha S, Chen J, Diao L, Dong X, Wallace MB, Killary AM, Frazier ML, Woodward TA, Wang J, Sen S. Circulating microRNAs in pancreatic juice as candidate biomarkers of pancreatic cancer. J Cancer 2014; 5: 696-705.

[8] Duan HF, Li XQ, Hu HY, Li YC, Cai Z, Mei XS, Yu P, Nie LP, Zhang W, Yu ZD, Nie GH. Functional elucidation of miR-494 in the tumorigenesis of nasopharyngeal carcinoma. Tumour Biol 2015; 36: 6679-6689.

[9] Wang Z, Zhang H, Zhang P, Li J, Shan Z, Teng W. Upregulation of miR-2861 and miR-451 expression in papillary thyroid carcinoma with lymph node metastasis. Med Oncol 2013; 30: 577.

[10] Yang B, Jia L, Guo Q, Ren H, Hu D, Zhou X, Ren Q, Hu Y, Xie T. MiR-564 functions as a tumor suppressor in human lung cancer by targeting ZIC3. Biochem Biophys Res Commun 2015; 467: 690-696.

[11] Liu X, Kong C, Zhang Z. miR-130b promotes bladder cancer cell proliferation, migration and invasion by targeting VGLL4. Oncol Rep 2018; 39: 2324-2332.

[12] Xie H, Zhan H, Gao Q, Li J, Zhou Q, Chen Z, Liu Y, Ding M, Xiao H, Liu Y, Huang W, Cai Z. Synthetic artificial "long non-coding RNAs" targeting oncogenic microRNAs and transcriptional factors inhibit malignant phenotypes of bladder cancer cells. Cancer Lett 2018; 422: 94-106.

[13] Xu T, Du XW, Hu JB, Zhu YF, Wu HL, Dai GP, Shu YM, Ouyang J. Anticancer effect of miR-96 inhibitor in bladder cancer cell lines. Oncol Lett 2018; 15: 3814-3819.

[14] Xu M, Li J, Wang X, Meng S, Shen J, Wang S, Xu X, Xie B, Liu B, Xie L. MiR-22 suppresses epithelial-mesenchymal transition in bladder can-

cer by inhibiting snail and MAPK1/Slug/vimentin feedback loop. Cell Death Dis 2018; 9: 209.
[15] Yang D, Du G, Xu A, Xi X, Li D. Expression of miR-149-3p inhibits proliferation, migration, and invasion of bladder cancer by targeting S100A4. Am J Cancer Res 2017; 7: 2209-2219
[16] Shehata SN, Hunter RW, Ohta E, Peggie MW, Lou HJ, Sicheri F, Zeqiraj E, Turk BE, Sakamoto K. Analysis of substrate specificity and cyclin Y binding of PCTAIRE-1 kinase. Cell Signal 2012; 24: 2085-2094.
[17] Thiselton DL, McDowall J, Brandau O, Ramser J, D'Esposito F, Bhattacharya SS, Ross MT, Hardcastle AJ, Meindl A. An integrated, functionally annotated gene map of the DXS8026-ELK1 interval on human Xp11.3-Xp11.23: potential hotspot for neurogenetic disorders. Genomics 2002; 79: 560-572.
[18] Huang MY, Xuan F, Liu W, Cui HJ. MINA controls proliferation and tumorigenesis of glioblastoma by epigenetically regulating cyclins and CDKs via H3K9me3 demethylation. Oncogene 2017; 36: 387-396.
[19] Forraz N, Pettengell R, McGuckin CP. Characterization of a lineage-negative stem-progenitor cell population optimized for ex vivo expansion and enriched for LTC-IC. Stem Cells 2004; 22: 100-108.
[20] Hua F, Sun J, Guo F, Yin S, Zhang Q, Zhang W, Liang W. Effect of downregulated histone deacetylase 2 expression on cell proliferation and cell cycle in cervical cancer. J Buon 2014; 19: 497-501.
[21] Hibino S, Saito Y, Muramatsu T, Otani A, Kasai Y, Kimura M, Saito H. Inhibitors of enhancer of zeste homolog 2 (EZH2) activate tumor-suppressor microRNAs in human cancer cells. Oncogenesis 2014; 3: e104.
[22] Taneera J, Fadista J, Ahlqvist E, Zhang M, Wierup N, Renstrom E, Groop L. Expression profiling of cell cycle genes in human pancreatic islets with and without type 2 diabetes. Mol Cell Endocrinol 2013; 375: 35-42.
[23] Zhou Q, Yu Y. Upregulated CDK16 expression in serous epithelial ovarian cancer cells. Med Sci Monit 2015; 21: 3409-3414.
[24] He J, Tang XF, Chen QY, Mai HQ, Huang ZF, Li J, Zeng YX. Ex vivo expansion of tumor-infiltrating lymphocytes from nasopharyngeal carcinoma patients for adoptive immunotherapy. Chin J Cancer 2012; 31: 287-294.